Paper 0119

Predictive Engine Simulations based on a novel DoE/RANS approach with coefficient tabulation

D. M. Nsikane[1], K. Vogiatzaki[1], R. E. Morgan[1]
[1]Centre for Automotive Engineering, University of Brighton, United Kingdom

ABSTRACT

Producing reliable in-cylinder simulations for quick turnaround engine development for industrial purposes is a challenging task. With the ongoing paradigm shift towards digital engineering, industry is forced to adjust its development and manufacturing processes away from prototyping and reliance on test bed results towards a virtual environment where optimization occurs before the actual hardware is available. In this work, an approach is presented, which can overcome one of the main disadvantages of RANS: the model coefficient tuning dependency. Using a Design of Experiments approach, it is shown that input parameters can be linked to ambient boundary conditions and therefore tabulated to eliminate lengthy tuning iterations between operating conditions.

1 INTRODUCTION

Digital product development, based on advanced numerical modelling, is progressively becoming an integral part of the design of modern energy systems. The breadth in available data and the new computing capabilities, along with advances in other areas such as artificial intelligence and automation are adding virtual design tool innovations that have the potential to change the nature of manufacturing itself. Testing future systems in a virtual environment is a more time and cost-effective way of design validation in comparison to conventional hardware-based methods. However, the reliability of virtual validation depends on the reliability of the virtual tools which therefore requires rigorous validation to a wide range of operating conditions. In diesel injection and combustion in Internal Combustion Engines (ICE's), this can be proven a challenging task due to the large range of scales and phases involved in fuel injection dynamics. Simulating the full spray combustion process from injection to combustion, in particular for thermodynamically extreme conditions (injection pressures reaching up to 300MPa) that modern systems operate at, is a challenging and computationally demanding task. These complex calculations might defy the purpose of using Computational Fluid Dynamics (CFD) as a time efficient virtual design tool. It is required that simulations keep up with the fast test bed results (400 Design of Experiments (DoE) points a day on a testbed). Using methods that "ignore" some of the scales of the problems under investigation (such as Reynolds-Averaged Navier-Stokes (RANS) and Large Eddy Simulations (LES)) can reduce the computational time but introduce new uncertainties. The numerical models use a range of parameters that encapsulate "unknown" or "unresolved" information at the sub grid scales. Determining which model coefficients have a significant impact on the performance measures of interest can be a daunting task. The common approach of changing one factor at a time is very often incorrect and misleading. This is due to multidimensional variable interactions which impact on the responses. An additional limitation in virtual tools comes from the difficulty in acquiring experimental data for validation based on real scale experiments. Most of the currently available quantitative data which can provide information up to the droplet detail are based on lab scale experiments that are simplifications of the real engines and represent isolated operating conditions. An example of one of the most recent fuel injection data sets are the data from the Engine Combustion Network (ECN) [1-3]. Their data is derived from a constant volume chamber. Experiments for a range of fixed pressures (50-150bar) and temperatures (300-1400K) are available. In a real engine though, where the piston is moving, a range of these conditions is present simultaneously. Hence, tuning the model constants based one set of data is misleading.

Table 1: Physical complexity versus experimental detail of the available experimental data

Parameter	ECN Spray A	RCM	Engine
Chamber volume	Constant	Changing	Changing
Charge temperature, pressure and density gradients	Low	Moderate	High
Swirl levels	Low	Moderate	High
Droplet impingement	No	No	Yes
Injector	Single-hole	Multi-hole	Multi-hole
Fuel	n-dodecane	Pump fuel	Pump fuel
Experimental control	High	Moderate	Low
Confidence in results	Very high	High	Moderate

2 METHODOLOGY

To address the problem of unreliable tuning for in-cylinder simulations, a comprehensive approach based on tabulation of the constants which paves the way for automation in in-cylinder CFD and use of machine learning techniques in the future is introduced. The methodology is in part inspired by the work done by Pei *et al* in [4, 5] and by the benefits tabulated chemistry has proven to have over solving complex chemical reactions in terms of computational efficiency. Starting from the conditions of a simplified environment of constant volume experiments (ECN Spray A) [6], coefficient matrices that correspond to individual operating points are derived. Then these coefficient matrices are used to extract a mapping between the trend in the value change of these coefficients and the underlying physical conditions. The next step is an inversion of the mapping process where areas of different physics were identified in progressively more complex configurations (Rapid Compression Machine (RCM) and Engine). A self-adjusted set of coefficients based on tabulation is introduced to correspond better to the changing conditions in the cylinder as the piston moves. Given the limitation of space in this paper, the focus will be on the first part of the process of how the coefficient matrix is derived while the automation for the application to a real engine will be presented in a follow up publication. Although the approach is currently implemented within the RANS context and simplified chemistry is used, extension to LES and more complex chemistry is straight forward.

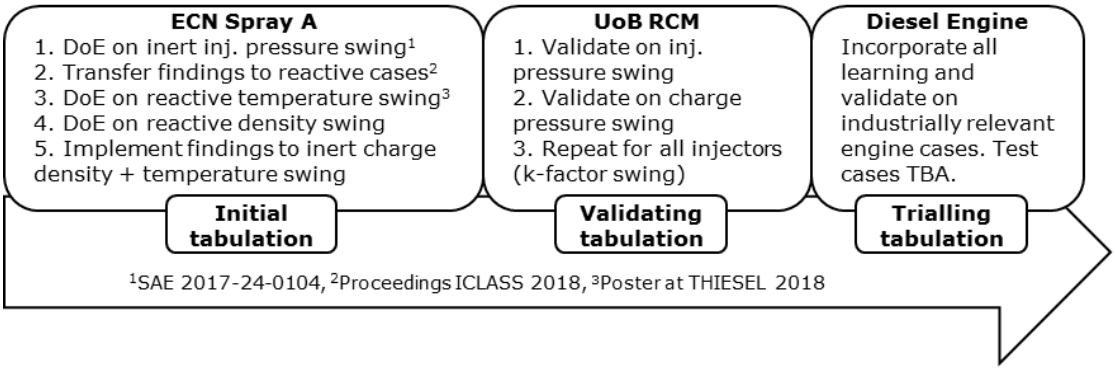

Figure 1: Framework Progression Outline

2.1 Selection of Experimental Data (Spray A for now and RCM for future)

2.1.1 ECN Test Data

The ECN offers a particularly rigorous dataset under various boundary conditions and injector configurations. For this work, a set of experiments commonly known as the ECN Spray A has been selected (see Table 2).

Table 2: Selection of ECN Spray A parametric variations

Key point	Charge Temp (K)	Charge Density (kg/m³)	Inj. Pressure (MPa)	Reactive (Yes/No)	Injector (#)	Available data
1	900	22.8	150	No	210677	Liquid & vapour penetration, axial & radial mass fraction and charge temperature distributions
2			100			
3			50			
4	1100	15.2	150			
5	1400	7.6				
6	750	22.8		Yes	210677 & 210370	For inj. #210677 Reactive vapour penetration, Lift-off-length, instantaneous & total heat release, absolute pressure For inj. #210370 Lift-off-length, total heat release, absolute pressure
7	800					
8	850					
9	900					
10	1000					
11	1100					
12	1200					
13	900	7.6			210370	
14	900	15.2				
15	1100	7.6				

The ECN Spray A configuration is defined as the diesel surrogate n-dodecane being injected vertically through a single-hole injector into a quiescent combustion chamber. Much effort has been put in to characterize the specifications of the injector and has been summarized in Table 3.

Table 3: ECN Spray A injector specifications [9]

Fuel injector nominal nozzle outlet diameter	0.090 mm
Nozzle K factor	K = 1.5
Discharge coefficient	C_d = 0.86
Fuel	n-dodecane
Fuel temperature at nozzle	363 K (90°C)

2.1.2 RCM Test Data

The available experiments have been conducted on a reciprocating RCM at the University of Brighton. The configuration (see Table 4) is based on an optically accessible converted Ricardo Proteus single cylinder engine [10]. This data set was selected because it offers a large optical access and considerably higher fuel injection frequencies than the ECN vessel. The experiments listed in Table 6 were conducted by Njere *et al* [11] with different injectors (see Table 5) that are relevant to the engine research community. The test matrix offers an overlap to the ECN data and incorporates relevant aspects like pump diesel, density & pressure gradients and moving parts. The biggest advantage, however, is the availability of injection pressures up to 2000bar which are highly relevant to the engine community, as these are approaching the trans-critical or even supercritical regime.

Table 4: RCM Hardware configuration

Compression Ratio	9:1
Charge pressures	Up to 8MPa
Charge temperatures	Up to 900K
Fuel	n-dodecane
Engine speed (Motored by dynamometer)	500rpm
Optical access	80mm height, Ø50mm at the ends

Table 5: Injector specifications

Injector	Flow rate (cc/min)	Number of Holes (#)	Nozzle Diameter (µm)	Cone Angle (deg)	k-factor (-)
A (Delphi)	770	7	130	155	2
B (Delphi)	860	8		156	1.5
C (Bosch 3601)	960		137	155	1.3
D (Bosch 3603					3.5

Table 6: Description of the available data at the defined key points

Key point	Inj. Pressure (MPa)	Fuelling (mm3)	Charge Pressure (bar)	Charge Temp (K)	Available liquid penetration Data	Available vapour penetration Data
1	200	65	84	~850K	A	-
2	160	36.31			A, B, C, D	B, C, D
3	140	36.71			A	-
4	100	35.31			A, B, C, D	B, C, D
5	60	34.86			A	-
6	200	45	50		A	-
7	160				A, C, D	D
8	140				A	-
9	100	25			A, B, C, D	B, C
10	200	65	66		A	D
11	140	45			A	-
12	100				A	-
13	180	60	79		A	B
14	160	50	73		A, B, C, D	B, C, D
15	60	20	40		A, B, C, D	B, C, D

2.2 Numerical Setup

The entire study is conducted in Ricardo Software's commercially available CFD package VECTIS. VECTIS is a RANS based code with a long history of extensive industrial use for ICE's and is therefore well validated [12]. The common sensitivity tests based on the grid resolution, time-step and parcel introduction rate were undertaken and have been reported in [13]. These settings can be carried over throughout the investigation concerning the ECN combustion vessel. When the results will be transferred to the RCM geometry, these numerical conditions will be re-evaluated. The selected sub models are listed in Table 7.

Table 7: List of selected sub models

Category	Selected Model
Turbulence Model	Standard k-ε [14]
Spray Injection Method	Blob (Single size)
Droplet Tracking method	Eularian-Lagrangian
Droplet Breakup Model	KH-RT with Levich switching criterion [15, 16]
Droplet Drag Model	Putnam [17]
Droplet evaporation	Spalding correlation [18, 19]
Phase interaction	Droplet-droplet & Droplet-turbulence (two-way coupling
Auto Ignition Model	Livergood-Wu model [20]
Combustion model	Ricardo's Two-Zone Flamelet (RTZF) [21]
Laminar Flame Speed Model	Metghalchi & Keck model [22]
Turbulent Flame Speed	Gülder equation [23]

2.2.1 Simulation constants of selected the sub model matrix

The selection of the sub models is followed by a detailed analysis of the model constants. These model constants are implemented into the sub models to account for physical processes that are either too time consuming to calculate, or the dynamics of the physical process is unknown. Either way, they significantly simplify the calculation which reduces the computational time. The downside is an inherent tuning dependency with subsequent questionable simulation results if the model is not tuned appropriately. Table 8 shows the selection of simulation constants which exhibit a non-negligible impact on the simulation. These 14 constants influence three areas: turbulence, combustion, droplet breakup and are listed together with their phenomenological significance and suggested range. This recommended value and/or range is either assigned by the original model author or by trialling ahead of implementation. Some initial conditions are not part of any models but are often unknowns and influential and have therefore been added to the sensitivity matrix.

Table 8: Selected simulation constants and their physical implication

Parameter	Range	Phenomenon	Group
Schmidt Number	0.6 – 1	Species Diffusivity	Turbulence Coefficients
Coefficient of Dissipation C_1 (-)	1.35 – 1.55	Production of Turbulence	
Coefficient of Dissipation C_2 (-)	1.65 – 1.9	Destruction of Turbulence	
Burning Velocity Coefficient A_0 (-)	0.3 – 1.5	Combustion	Combustion Coefficients
Auto-Ignition Coefficient c_{ig} (-)	0.3 – 1.2	Ignition	
Turbulent Flame Speed Multiplier α_{turb} (-)	0.1 – 3	Turbulent Combustion	
Drag scaling factor A_{drag} (-)	0.2 – 1.5	Liquid/Gas Momentum Transfer	Droplet Breakup Coefficients
KH B_1 – Constant (-)	1 – 40	Primary Atomization	
KH B_0 – Constant (-)	0.3 – 0.8	Primary Atomization	
RT C_{RT} – Constant (-)	0.3 – 2	Secondary Atomization	
RT - C_3 – Constant (-)	0.3 – 5.3	Secondary Atomization	
Levich A_{bu} – Constant (-)	5 – 12	Primary/Secondary Atomization	
Initial droplet diameter D_0 (µm)	60 – 90	Droplet Introduction	Initial conditions
Initial Half Cone Angle α_{cone} (deg)	2.5 – 7.5	Initial Dispersion	

2.3 Design of Experiment

The general goal of an "experiment" is to identify the influence of input parameters on output parameters within a system, highlight the sensitivity of the system towards changing conditions or find a combination of input parameters which produce a desired output. DoE is a tool which, given an appropriate matrix, can use a statistical approach to analyse input parameters, visualize their interactions and sensitivities and optimize towards a desired

output. Among other areas, DoE is a powerful and popular tool in test bed engine calibration, however in the current paper is used to drive the investigation of in-cylinder CFD simulations.

2.3.1 Simulation Design Matrix

By running a statistically relevant number of simulations with the simulation constants presented in Table 8, a multidimensional stochastic process model (SPM) is produced. This can then highlight influential constants, their sensitivities and impact on macroscopic spray characteristics like liquid & vapour penetration, heat release and lift-off-length. A value of 10 simulations per DoE variable is considered statistically relevant. This means that for the inert cases, which ran with 10 DoE variables, 100 simulations per case were run. Respectively, 140 simulations per charge temperature condition were run in the reactive cases. The DoE tool assigns each simulation with a unique combination of the parameters from Table 8 within the defined range and simultaneously optimally distributes them in the design space.

2.3.2 Simulation Comparison Metric

The Root-Mean-Square-Error (RMSE) method is selected to automate the quality assessment of the simulations. With this method, the difference of absolute values is calculated at each time-step, summed up and then normalized over the number of time-steps (eq. (1) in Table 9). Like this, the entire difference between the curve propagations is considered. To avoid skewing the error value, it is important to exclude regions of high transients. While comparing transient behaviour is just as important, they can lead to the exclusion of otherwise good simulations due to unreasonably high errors in the injection ramp up or SoC. These highly transient zones are best investigated manually.

Table 9: Mathematical background for RMSE approach

Case	Time-step	Metric Value	No. of time-steps
Experiment	t	$x_{1,t}$	n_t
Simulation		$x_{2,t}$	

$$RMSE = \sqrt{\frac{\sum_{t=1}^{n_t}\left(x_{1,t} - x_{2,t}\right)^2}{n_t}} \qquad (1)$$

2.3.3 DoE Optimization

There are too many parameter combinations which could lead to a matching solution to be analysed manually. To narrow down viable solutions, a built-in mathematical optimizer is equipped with user defined target conditions. The optimizer creates a pareto diagram and compiles a list combinations of input parameters which fulfil the target condition (~15 options). In this work, the target condition is a low error trade-off between the liquid penetration, vapour penetration, heat release and lift-off-length. Since there is not a single solution for these criteria, the optimizer will provide multiple solutions. To further narrow down the number of solutions and exclude non-physical combinations, the remaining few solutions (~5 options) are scrutinized by investigating microscopic characteristics like droplet sizes, their transient regions of injection ramp up and start-of-combustion and finally, how they behave to changing boundary conditions. A quality criterion would for example be that at discrete temperature increase (with unchanged density) a simulation setup at each condition can be found that together exhibit a sweep in values which are related to a temperature swing. This analysis is carried out for every constant at every test condition and a final best option selected.

2.3.4 The necessity of DoE

When faced with the challenge of matching a simulation to experimental data, it is customary practice to conduct a parametric study [24], which usually consists of single parameter swings. This section will show an example how this widespread approach can be misleading. The KH-time constant B_1 has been extensively investigated and is among the favourite tuning constants for engineers and researchers to tweak unsatisfactory results. Without going into much detail, B_1 can be summarized to scale the rate at which the droplets in the primary breakup shrink before being passed on to secondary breakup. Below in Figure 2, a discrete swing of B_1 between the ranges from Table 8 is shown. A low B1 (rapid droplet shrinking) has the effect of reducing the drop size from inlet condition of ~77µm to 2.5µm within 5mm from the nozzle exit. Some of these small droplets at the periphery of the spray complete their evaporation process and fulfil the requirements for them to combust, yielding a reduced lift-off-length. Some droplets, however, linger and only evaporate much later (~12mm) due to the secondary breakup effect from C_3, the RT-equivalent timescale of B_1. A high B1 has the opposite effect on lift-off-length due to the droplets undergoing retarded breakup. The droplet size distribution between 3 and 9mm have widened significantly indicating that while some droplets are shrinking faster, the bulk is breaking up slowly. Again, this is a result of the competing RT-influence on droplets breaking up at the periphery of the liquid core. Because of this slow breakup, the lift-off-length is postponed by 7.5mm in comparison to a low B_1. All B_1 values have no apparent effect on vapour penetration, which is also often a comparison metric. Hence, the user may be convinced that the used value is the correct one, while other metrics are severely influenced.

The point here is that often B_1 is simply changed to adjust liquid penetration length without considering neither the implications nor the complexity of the interactions with other physical processes. While the below figure only shows the effect of B_1, all other constants in Table 8 produce individual responses on every comparison metric. Faced with the scale of this problem, it should become clear that a more sophisticated approach to visualizing the effect of each constant on specific metrics is necessary to guide the simulation tuning process.

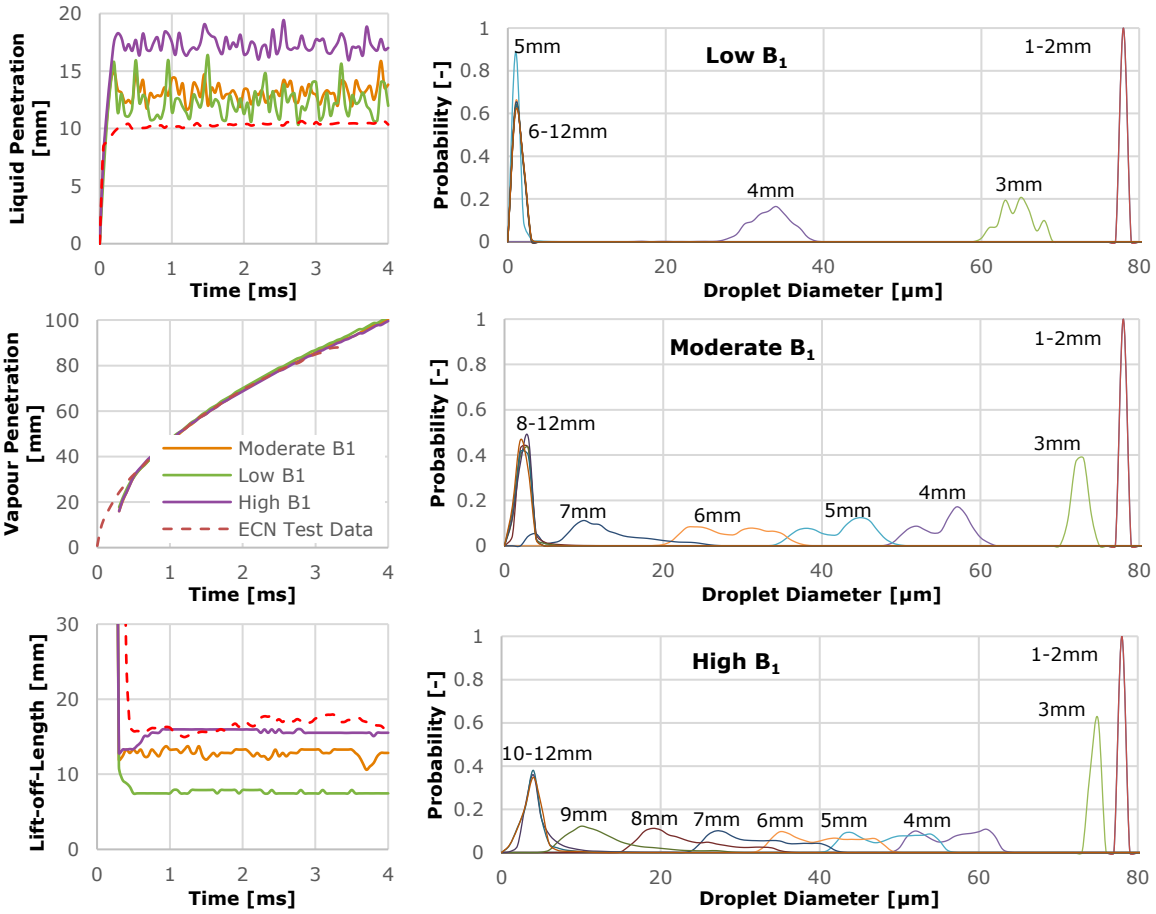

Figure 2: The effect of a discrete swing of KH-time constant B_1 on multiple comparison metrics

2.4 Computational effort

A similar approach on ECN Spray A conditions with RANS combined with Global Sensitivity Analysis (GSA) by Pei *et al* in [4] reported an average of 75 wall clock hours per simulation on 16 cores. Another study, also on the same conditions, by Som *et al* in [25] reported a wall-clock time for 2ms injection duration of 18hrs (RANS) and 150hrs (LES) for reactive cases and 2hrs (RANS) and 20hrs (LES) for non-reactive cases on 16 cores. The significantly longer simulation duration is the consequence of the use of detailed and reduced chemical kinetics solvers. The average duration per simulation over a 4ms injection duration on 20 cores Intel(R) Xeon(R) CPU E5-2650 v3 CPUs with 2.30GHz in this work is around 2hrs for the inert and 7hrs for the reactive cases, however with a simplified chemistry solver. This simplified setup however, can produce high quality results as will be shown in section 3. This brief comparison highlights the potential time benefit of using simplified models over detailed solvers, though correct tuning becomes of utmost importance.

3 INDICATIVE RESULTS OF REACTIVE CASES

The scope of this paper is to underline the relevance of the DoE methodology and to lay the groundwork for future input parameter tabulation. Due to space limitation, the following section will show only selected indicative results obtained when utilizing the DoE approach for reactive ECN Spray A variations.

3.1 Producing a stochastic process model for each charge temperature condition

The process outlined in section 2.3.3 is followed on low, medium and elevated temperature conditions (cases 7, 9 & 12 from Table 2. After running 140 simulations for a range of coefficient combinations, the RMSE's between the calculated and experimental results of the comparison metrics are calculated. This map of correlations between 140 individual input matrices and their corresponding output error matrices is bundled into a stochastic process model. An example visualisation of this model of the 900K baseline case is provided in Figure 3. Each row represents the error sensitivity of a target metric towards a change in the respective simulation constants in the columns. The numbers indicating the constant values and RMSE at the boundaries of the fields have been removed for clarity and to support a qualitative narrative. The significance of the constants on the x-axis are mentioned in Table 8. Each individual field shows how the error between simulation and experimental data would behave when the constant is adjusted. For example, refer to the column of B_1. The model shows that a discrete increase of B_1 leads to reduced lift-off-length-error while simultaneously increasing the liquid penetration error. The effect on vapour penetration ad heat release error is marginal. The effect of this discrete B_1 swing in shown previously in Figure 2. However, should B_1 be altered in the model, all 13 remaining error curves will be affected.

This means that the change of a single constant like B_1 could be countered by another and appear to have no effect on the overall outcome on one metric while affecting a completely different area of the simulation. This figure shows the complex nature of the multidimensional interactions between the simulation constants and highlights the flaws of a discrete constant tuning approach.

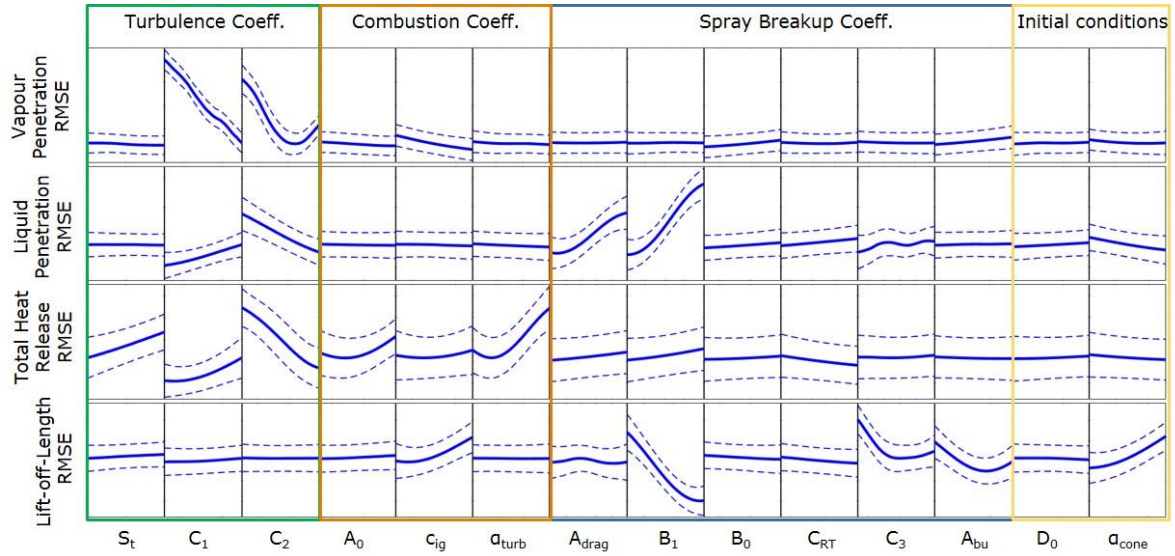

Figure 3: Stochastic process model showing error sensitivity of all 14 variables within their ranges

3.2 DoE Best Match for three reactive cases

Figure 4 shows the simulated vapour penetration, rate of heat release and total heat release against the ECN data at 800K (l), 900K (m) and 1200K (r). A discrete swing in charge temperature is not expected to have much impact on the vapour penetration if charge density, which is the dominating factor, is held constant. Accordingly, the used turbulence coefficients can remain unchanged between the cases. In comparison to the inert cases investigated in Nsikane *et al* in [13], both C_1 and C_2 are raised to accommodate combustion induced turbulence. At the time of this study, there was no available liquid penetration data for the reactive cases. However, based on Pickett *et al* in [6], it is justified to use the inert liquid penetration as a guide because the impact of downstream combustion on near nozzle droplet breakup is negligible. The optimization of the reactive 900K case showed strong similarity for the majority of breakup constants to the inert 900K case setup found in Nsikane *et al* in [13]. It was therefore decided to run all three cases with identical spray breakup coefficients as found in the inert case.

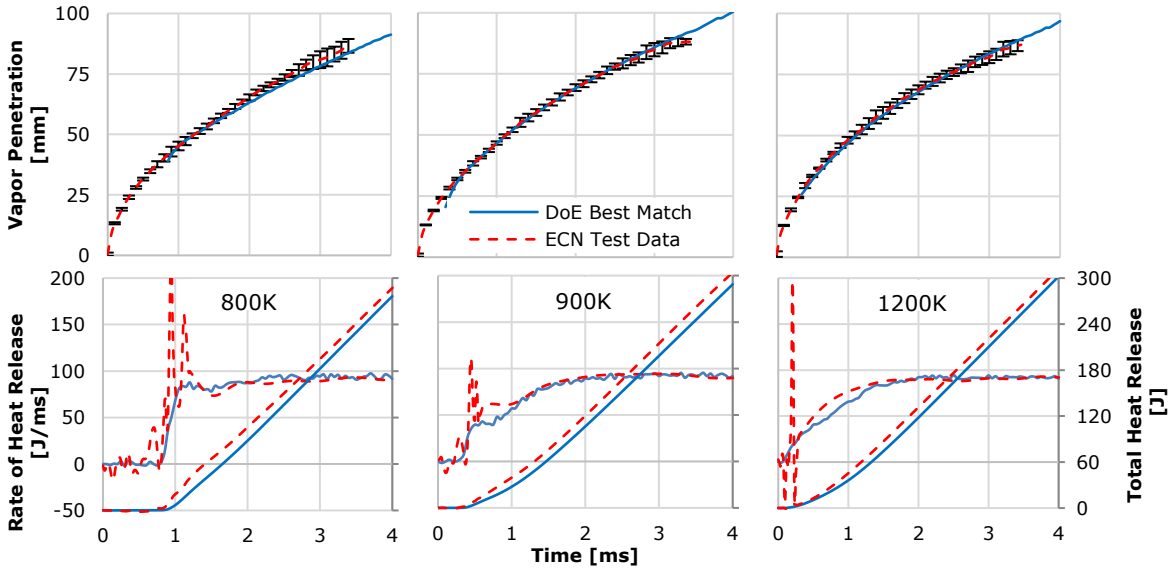

Figure 4: Simulated liquid penetration, vapour penetration, ROHR and AHR against exp. data at 800K (l), 900K (m) and 1200K (r)

A second effect that can be observed in Figure 4 is the clear advancement of start-of-combustion with rising temperatures. This characteristic trend is captured well in the simulations. The mismatch of the rate of heat release spikes trailing the start-of-combustion can be explained by the use of the simplistic Livengood-Wu auto-ignition model (simple chemistry model), which is not ideal to handle what are thought to be local premixed ignition events. The following combustion progression, including the areas of rise and stagnation of rate of heat release are captured well.

3.3 Input parameter trends required for matching experimental data

To arrive at the matches in Figure 4 we observed a non-linear progression of some coefficients. As an example, we show the initial droplet sizes and the auto ignition coefficient c_{ig} in Figure 5. The absolute values on the Y-axes are not disclosed due to confidentiality constraints. To hold the density constant while increasing the temperature in the constant volume chamber, the chamber pressure is adjusted. The effect of different ambient chamber pressures in experimental observations has been well reported, for example by Crua *et al* in [26]. Injecting liquid droplets into elevated ambient pressures significantly accelerates droplet breakup in the near nozzle region. When simulating the droplet injection with the simple blob model like in this setup, this complex breakup process can be replicated by introducing smaller droplets. Based on this reasoning, the initial droplet sizes are reduced with increasing chamber pressure (see Figure 5). The exact physical process behind the sensitivity of the augo-ignition coefficient is yet to be fully understood, but at this point it can be stated that without user intervention, the magnitude of the advancing of the start-of-combustion would not be replicated accurately.

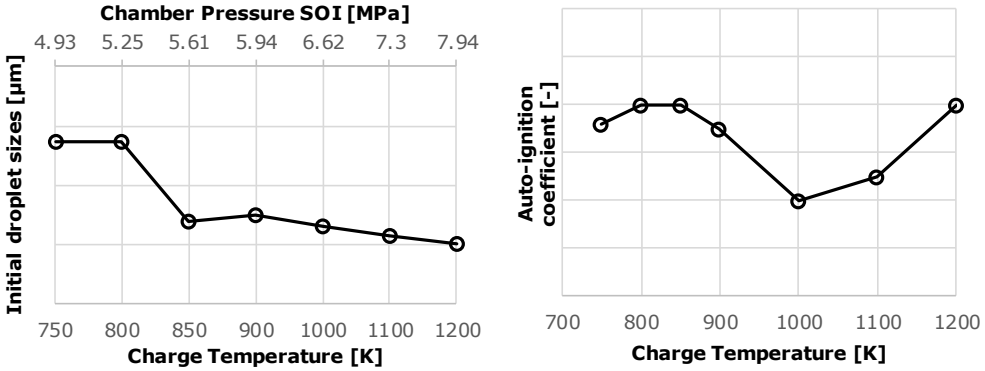

Figure 5: Trend of the required initial droplet sizes and auto ignition coefficient to achieve matching simulations

3.4 Results of initial tabulation

In the next step, the four validation cases (cases 6, 8, 10 and 11 from Table 2) were run with the setup derived from the DoE cases. This means turbulence and spray breakup coefficients, as well as initial conditions remained unchanged, while the auto-ignition coefficient and the initial droplet sizes followed the tabulation from section 3.3. The results of these simulations are shown in Figure 6. The simulations of the cases with charge temperatures greater than 800K show correlations in vapour penetration, accumulated & rate of heat release and start-of-combustion with similar quality to the DoE key points in Figure 4. Only the 750K case shows some deficiencies replicating the initial rate of heat release.

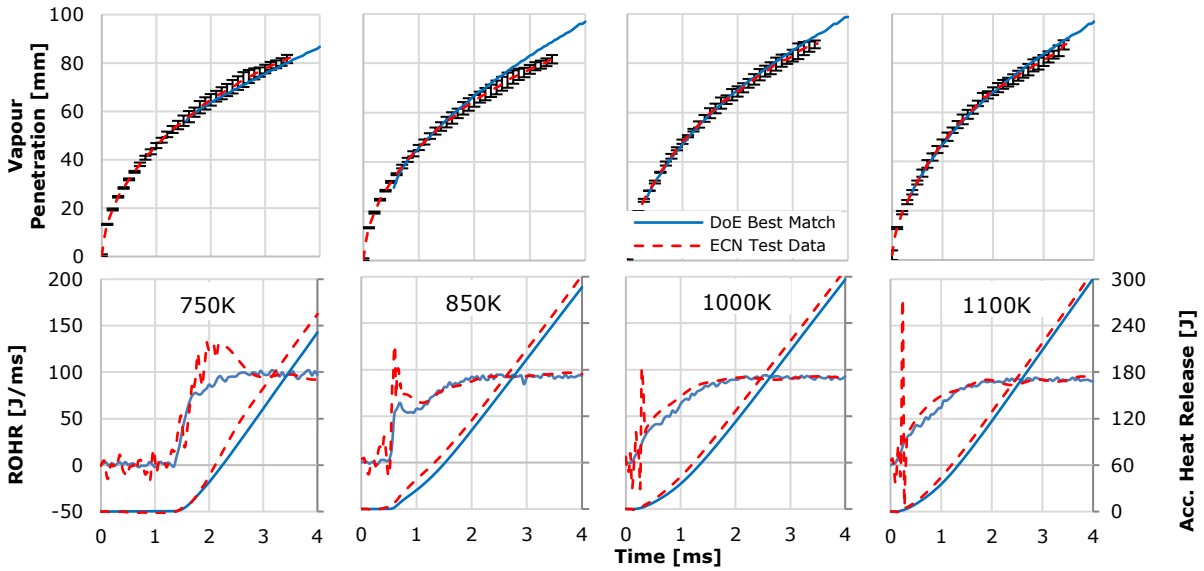

Figure 6: Simulated vs experimental liquid & vapour penetration, ROHR and accumulated HR at the remaining charge temperature conditions

A final quality assessment of the simulation consists of comparing the lift-off-length and liquid penetration. Due to the different definitions of lift-off-length between the simulations and the experiments this was only a qualitative comparison. In this work, the lift-off-length is defined as the furthest axial location of with threshold of 0.5 of the combustion progress variable. The ECN measures the lift-off-length using OH* chemiluminescence by finding the point of 50% rise of the chemiluminescence to its peak value at the leading edge of the flame.

Figure 7 shows a hyperbolic decrease in lift-off-length with increasing charge temperature. This qualitative progression is matched well. An action point here is to define an appropriate correlation between the OH*

definition and combustion progress variable definition of lift-off-length for simulation which do not use a detailed chemistry solver. The liquid penetration can at this point only be compared to Spray A experiments conducted at inert conditions. The simulated 900K and 1200K cases match their inert counterpart well. Towards the lower end of the temperature range, a clear deviation is visible indicating a strong sensitivity of either the constants or of numerical origin. The source of this deviation will be subject to future investigation.

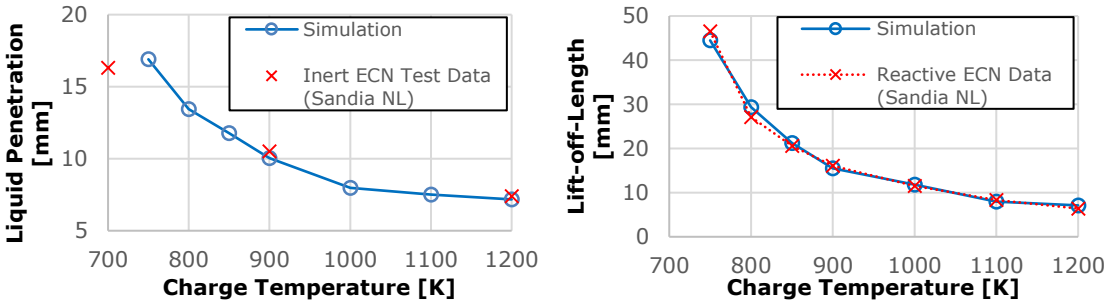

Figure 7: Simulated versus experimental liquid penetration and lift-off-length at all charge temperature conditions

4 CONCLUSION

Producing reliable in-cylinder simulations for quick turnaround engine development for industrial purposes is a challenging task. With the ongoing paradigm shift towards digital engineering, industry is forced to adjust their development and manufacturing processes away from prototyping and reliance on test bed results towards a virtual environment and optimization before hardware is available. To facilitate this shift into the virtual world, computational methods must become more sophisticated and reliable. With increasing computational power, approaches like DNS and LES have become more affordable, but only show their superiority over RANS in microscopic and research-oriented environments or development of more radical R&D concepts. This work argues, that if given appropriate tuning, RANS can provide high quality results for industrially relevant metrics in a fraction of the time. These metrics include matching macroscopic spray characteristics, start-of-combustion, heat release and emissions. To achieve reliable results, however, the dominating disadvantage of heavy tuning dependency of RANS must be overcome. In this publication, a methodology is proposed, in which Design of Experiment can be used to produce an input parameter map which in turn can be used for parameter tabulation following the concept of chemical kinetics tabulation. The current selection of input parameters faces two main problems: 1) the definition of the values follows no standardized structure because their significance is rarely understood and 2), the simulation constants are usually fixed across the entire computational domain. It is shown here, that some simulation constants are sensitive to changing boundary conditions. Changing boundary conditions are prone to happen in real engine operating conditions with a moving cylinder and combustion processes. Therefore, instead of treating input parameters as fixed quantities, they should change dynamically with the changing boundary condition. This of course has the consequence that the user no longer has control over the defined values meaning they must be predefined and well validated.

In the indicative results in section 3, an outtake of this work is shown. Three selected reactive charge temperature conditions are selected. At each charge temperature condition, the DoE methodology is applied until a single set of parameters is found which can replicate all metrics to a satisfactory standard. An analysis of the matrix of the input parameters show an interesting pattern. While initial conditions, breakup and turbulence coefficients can remain unchanged, the initial droplet size and some combustion model variables cannot. Interpolating and extrapolating the values to the remaining four charge temperature conditions provided a good correlation for all cases, increasing the confidence in this approach.

Although the approach shown here is currently implemented within the RANS context and is tailored to RS VECTIS, an implementation in other codes or even in an LES framework is straight forward.

ACKNOWLEDGEMENTS

The authors would like to acknowledge the high-quality experiments conducted by Cyril Crua and his team at the University of Brighton and the participants of the ECN, particularly the Sandia National Laboratories. Further, the authors would like to acknowledge the support by Kenan Mustafa, Nick Winder and Andrew Ward from Ricardo Innovations. VECTIS support was provided by Evgeniy Shapiro, Nick Tiney and Irufan Ahmed from Ricardo Software and nCal software assistance provided by Justin Seabrook. The authors would also like to thank the UK's Engineering and Physical Science Research Council support through the grant EP/P012744/1.

REFERENCES

1. L. Pickett, G.B., R. Payri, *Engine Combustion Network*. 2014: http:// www.ca.sandia.gov/ecn
2. Bardi, M., et al., *ENGINE COMBUSTION NETWORK: COMPARISON OF SPRAY DEVELOPMENT, VAPORIZATION, AND COMBUSTION IN DIFFERENT COMBUSTION VESSELS.* 2012. **22**(10): p. 807-842.

3. Meijer, M., et al., *ENGINE COMBUSTION NETWORK (ECN): CHARACTERIZATION AND COMPARISON OF BOUNDARY CONDITIONS FOR DIFFERENT COMBUSTION VESSELS.* 2012. **22**(9): p. 777-806.
4. Pei, Y., et al., *Engine Combustion Network (ECN): Global sensitivity analysis of Spray A for different combustion vessels.* Combustion and Flame, 2015. **162**(6): p. 2337-2347.
5. Pei, Y., et al., *Global Sensitivity Analysis of a Diesel Engine Simulation with Multi-Target Functions*. 2014, SAE International.
6. Pickett, L.M., et al., *Comparison of Diesel Spray Combustion in Different High-Temperature, High-Pressure Facilities.* SAE International Journal of Engines, 2010. **3**(2): p. 156-181.
7. Bardi, M., et al., *Engine Combustion Network: Comparison of Spray Development, Vaporization and Combustion in Different Combustion Vessels.* 2012. **22**(10): p. 807-842.
8. Meijer, M., et al., *Engine Combustion Network (ECN): Characterization and Comparison of Boundary Conditions for different Combustion Vessels.* Atomization and Sprays, 2012. **22**(9): p. 777-806.
9. Network, E.C. *"Spray A" and "Spray B" Operating Conditions*. 2016 [cited 2017 26/02/2017].
10. Crua, C., *Combustion processes in a diesel engine*, in *CEM*. 2002, University of Brighton, UK: http://eprints.brighton.ac.uk/1161/.
11. Njere, D.O., *Optical characterisation of high pressure diesel fuel injectors*, in *CEM*. 2015, University of Brighton: http://eprints.brighton.ac.uk/id/eprint/14206.
12. Li, G., S.M. Sapsford, and R.E. Morgan, *CFD Simulation of DI Diesel Truck Engine Combustion Using VECTIS*. 2000, SAE International.
13. Nsikane, D.M., et al., *Statistical Approach on Visualizing Multi-Variable Interactions in a Hybrid Breakup Model under ECN Spray Conditions.* SAE International Journal of Engines, 2017. **10**(5).
14. Jones, W.P. and B.E. Launder, *The prediction of laminarization with a two-equation model of turbulence.* International Journal of Heat and Mass Transfer, 1972. **15**(2): p. 301-314.
15. Lefebvre, A., *Atomization and Sprays*. 1988: Taylor & Francis.
16. Beale, J.C., *Modeling fuel injection using Kelvin-Helmholtz/Rayleigh-Taylor hybrid atomization model in KIVA-3V*. 1999: University of Wisconsin--Madison.
17. Putnam, A., *Integratable Form of Droplet Drag Coefficient*. 1961, J. Am. Rocket Soc. p. 1467-4798.
18. D.B., S., *The Combustion of Liquid Fuels*, in *4th Symposium (International) on Combustion*. 1953, Williams & Wilkins: Baltimore. p. pp. 847-864.
19. Chin, J.S.a.L., A.H., *The Role of the Heat-up Period in Fuel Drop Evaporation.* Int. J. Turbo Jet Engines, 1985. **vol. 2,**: p. pp. 315-325.
20. Livengood, J.C. and P.C. Wu, *Correlation of autoignition phenomena in internal combustion engines and rapid compression machines.* Symposium (International) on Combustion, 1955. **5**(1): p. 347-356.
21. Chen, C., M.E.A. Bardsley, and R.J.R. Johns, *Two-Zone Flamelet Combustion Model*. 2000, SAE International.
22. Metghalchi, M. and J.C. Keck, *Burning velocities of mixtures of air with methanol, isooctane, and indolene at high pressure and temperature.* Combustion and Flame, 1982. **48**: p. 191-210.
23. Gülder, Ö.L., *Turbulent premixed flame propagation models for different combustion regimes.* Symposium (International) on Combustion, 1991. **23**(1): p. 743-750.
24. Dempsey, A.B., et al., *Comparison of Quantitative In-Cylinder Equivalence Ratio Measurements with CFD Predictions for a Light Duty Low Temperature Combustion Diesel Engine.* SAE Int. J. Engines, 2012. **5**(2): p. 162-184.
25. Som, S., Senecal, P.K., Pomraning, E., *Comparison of RANS and LES Turbulence Models against Constant Volume Diesel Experiments*, in *ILASS Americas, 24th Annual Conference on Liquid Atomization and Spray Systems*. 2012: San Antonio, TX.
26. Crua, C., M.R. Heikal, and M.R. Gold, *Microscopic imaging of the initial stage of diesel spray formation.* Fuel, 2015. **157**: p. 140-150.